CI&CEQ
Chemical Industry & Chemical Engineering Quarterly

Available online at
Association of the Chemical Engineers of Serbia AChE
www.ache.org.rs/CICEQ

*Chem. Ind. Chem. Eng. Q.* 32 (1) 1–13 (2026) CI&CEQ

PRAKASH CHAKRAPANI[1]
PRAKASH JAYARAMAN[2]

[1]Department of Automobile Engineering, School of Engineering and Technology, Surya Group of Institutions, Anna University, Tamilnadu, India.

[2]Department of Mechanical Engineering, School of Engineering and Technology, Surya Group of Institutions, Anna University, Tamilnadu, India

# SLOT MILLING OF AA7075 REINFORCED WITH NANO SILICON CARBIDE PARTICLES – AN EXPERIMENTAL AND FINITE ELEMENT APPROACH

## Highlights

- The aluminum nanocomposite is fabricated, and machinability studies are performed.
- The nSiCp reinforcement improves the mechanical characteristics of the AA7075 material.
- Experimental slot milling is performed and cutting force, chip morphology studies are carried out.
- Slot milling is simulated using 3D FEM and the Experimental Vs 3DFEM correlation studies are done.
- The influence of cutting parameters on machinability of the nanocomposite is evaluated.

## Abstract

*In the current trend, industries prefer to optimize machining processes using finite element-based machining simulation techniques. Aluminum alloy 7075 (AA7075) strengthened with nano silicon carbide particles (nSiCp) is utilized by industries as they exhibit good physical and mechanical properties. Slot milling is the essential machining operation to convert the component to the designed shape and size. However, excellent knowledge is required in selecting the appropriate machining parameters such as cutting velocity, feed, and cutting tool material to ensure the quality of the components milled. In this research work, slot milling operation is carried out in the sample plates of AA7075 fortified with nSiCp content to 1.5% of the weight. A 3D finite element model (3D FEM) is developed using ABAQUS software for simulating slot milling operations to understand the influence of machining parameters on cutting forces, chip formation, and chip morphology. The cutting force signals predicted by 3D FEM correlates 85 to 90% with experimental data. The maximum shear stress of 175 MPa and Von Mises stress of 459 MPa were observed at the tool-workpiece interface. This validated 3D FEM facilitates to visualize and investigate the milling process and assists in selecting appropriate machining parameter settings. The effects of cutting velocity and feed on cutting forces, chip characteristics, stress, and chip formation are reported.*

*Keywords: Aluminum nanocomposite, slot milling, 3D FEM, cutting forces, chip morphology.*

SCIENTIFIC PAPER

UDC 621.9:669.71:66.017:004

## INTRODUCTION

The machinability of the aluminum nanocomposite investigated in this research work is an aluminum-based metal matrix composite (MMC) reinforced with nano SiC particles (<100 nm) to improve the mechanical properties of AA7075 based on the requirements in modern industries. These MMCs are extensively utilized by the automo-bile and aircraft industries due to their intrinsic mechanical properties when compared to steel such as being lighter in weight, ductility, good stiffness, fracture toughness, and corrosion resistance even at extreme operating conditions. It attracts the attention of researchers and makes it necessary to investigate the machinability of aluminum-based nanocomposites [1-3]. It has been projected that, by 2025 the increase in utilization of aluminum in a car will reach 250 kg from 150 kg as of now [4].

The aluminum-based MMCs reinforced with SiC particles have potential applications in the aviation and transport fields, bearings, fins of aircraft fuselage, struts of avionics systems and aero engine compressor blades [5],

Correspondence: P. Chakrapani, Department of Automobile Engineering, School of Engineering and Technology, Surya Group of Institutions, Anna University, Vikiravandi – 605652, Villupuram District, Tamilnadu, India;
Email: prakashc@suryagroup.edu.in
Paper received: 26 August, 2024
Paper revised: 19 March, 2025
Paper accepted: 24 March, 2025
https://doi.org/10.2298/CICEQ240826006C

brake wheels of four-wheelers and high-speed trains [6]. The milling process is mostly utilized to bring the raw material / semi-finished product to the designed shape and size. However, machining defect-free products/components with good quality is challenging in aluminum nanocomposite due to the nSiCp reinforcement in aluminum nanocomposite, which is greatly influenced by the machining parameters selected and the machining conditions [7]. The challenging issues in the milling of aluminum-based MMCs are dimensional inaccuracy, chip built-up edge, unstable cutting forces due to reinforcement material (nSiCp), higher cutting forces, surface roughness, stress concentration, accelerated tool wear, exit burr formation, surface finish and reduction of fatigue life, etc. Hence, ensuring the dimensional accuracy, quality, and reliability of the machined components by eradicating these damages caused while machining is very much essential. Moreover, it is also mandatory to explore the basics of machining the MMCs by investigating the importance of the volume and distribution of the nano SiC particles on the damage mechanism of MMC, the interaction of the mill tool with SiC particles, and the effect of machining parameter combinations (feed rate, depth of cut, cutting velocity, etc.) on dimensional accuracy, quality of the machined surface and ease in machinability. This motivates the engineers, researchers, and industries to investigate on milling of aluminum-based MMC to understand the effects of SiC reinforcement in its machinability [8].

To eradicate the machining difficulties experimental studies are mandatory which is time-consuming and highly expensive, particularly at extensive machinability metrics (i.e. combination of machinery, tool material, tool geometry, machining parameters, and machining environment selected for machining studies) [9]. However, interpreting the experimental results highly depends on the quality of the machinery and data acquisition equipment used. Moreover, it is essential to have a complete understanding of the behavior of metal matrix composites while machining under different machining parameter combinations, which could optimistically ease the machining operations. Hence, the researchers and industries wish to utilize 3D FEM for investigating the machining of MMCs. Using 3D FEM the complex milling process is simulated in three dimensions to predict the cutting forces and cutting stress and to visualize for understanding the chip formation process.

Bhuvanesh *et al.* [10] reported the influence of machining parameters on surface roughness while performing slot milling in aluminum-based hybrid composite strengthened with SiC and $B_4C$ materials. The reduction in plastic deformation is observed with the increased percentage of reinforcement particles while machining. Hence, it is suggested to perform slot milling operations at larger cutting velocities and minimum feed rates to remove the reinforcement material easily and to achieve a good surface finish. Ma *et al.* [11] performed the experimental milling in aluminum alloy 7075 and reported the cutting forces, stress, and chip morphology. The finite element analysis (FEA) simulation studies are also made and the results were correlated with the experimental findings and seem to be similar. Davoudine-jad *et al.* [12] simulated the slot milling process using a 3D FE model for different machining parameter combinations and reported the cutting forces, chip morphology, cutting temperature, and stress obtained from experimental and finite element (FE) studies.

Raghuvaran *et al.* [13] reviewed the mechanical properties of aluminum-based MMC. It is reported that AMCs find extensive applications in the aerospace and automobile industries and thereby they replace conventional metals and materials. Reinforcement of SiC 10% of weight with AA7075 increases the tensile strength of the composite by 9.67% which creates interest among researchers. Cui *et al.* [14] established a 3D FEM using ABAQUS/Explicit and simulated the milling operation in aluminum alloy 7075-T7451. The authors also reported the cutting force data and chip morphology. Umer *et al.* [15] investigated the subsurface damages caused while machining the aluminum-based MMCs using a 2D FE model. The researchers revealed the machined surface damages such as damage depth, particle debonding, and the effects of cutting velocity and feed on the quality of the machined surface. The researchers also developed 2D micromechanical and 3D equivalent homogeneous models to simulate the orthogonal cutting of aluminum-based (Al359) SiC-reinforced MMC. The EHM model proves its ability in predicting and simulating the cutting process effectively by Umer *et al.* [16]. Zhou *et al.* [17] developed a 2D FEM and simulated the orthogonal cutting process. The researchers reported the effects of machining parameters on residual stress, surface roughness, dimensional accuracy, and shape.

Prakash *et al.* [18] developed a 3D FEM to simulate the slot milling process in unidirectional Carbon fiber-reinforced polymer composites. The investigation reveals how the machining parameters such as cutting velocity and feed influence cutting forces, stress, chip formation, chip morphology, and machining-induced damages. The developed 3D FEM also assists in selecting appropriate machining parameter settings to enhance the machining quality and dimensional accuracy. Prakash *et al.* [19] utilized the developed 3D FEM from the earlier research work and simulated the high-speed milling of AA7075 Reinforced with nB4Cp. The 3D FEM-based milling simulations suggested milling the MMC with higher cutting velocity and at a lower feed rate. Pedroso *et al.* [20] concisely summarised the utilization of FEA strategies for predicting the machining process in INCONEL material and briefed the recent advancements in machining simulations from 2013 to 2023. The review work carried out by the authors revealed the necessity to investigate more for developing new 3D FEMs for enhancing their accuracy and reliability.

Dodla *et al.* [21] studied conventional and ultrasonic vibration-assisted machining of aluminum alloys, titanium alloys, and Inconel – 718 materials. Numerical methods of both machining techniques reported the cutting forces, thermal effects, and chip morphology. The authors suggested utilizing UVA machining to reduce machining forces and machining-induced damages. Deshmukh *et al.* [22] reported a brief review on the machining of aluminum-

based Metal Matrix Composites which guides the researchers to work on cutting tool methodology. The authors reported the recent advancements in the machining of MMCs in their review article. The authors also highlighted the various types of MMCs available and their inherent mechanical behaviors which suit specific industry applications and also create the interest for the researchers to evolve new hybrid MMCs. Liangchi *et al.* [23] reviewed the recent advancements in modeling the machining of fiber-reinforced and particulate-reinforced composites. The review reveals that the accuracy and reliability of the numerical model highly relies on the correctness of constitutive models incorporated in the FEM.

Prakash *et al.* [24-30] have presented a recent work focusing on developing 3D FEM and simulated the drilling and slot milling operation in GFRP, CFRP composites, Aluminum-based MMCs, and investigated the influence of cutting velocity and feed on cutting forces, stress, chip formation, and chip morphology. These researchers provided insight to understand and visualize the drilling and slot milling process in those composites. The experimental findings and 3D FE predictions are excellent in similarity and the developed 3D FE model is novel and reliable in simulating and predicting the optimum machining parameter settings. Prakash Jayaraman *et al.* [31,32], the co-author of this fabricated and investigated the mechanical properties of aluminum nanocomposite, also studied the quality of the holes drilled in the fabricated composite. The researchers suggested AA7075 with 1.5% nSiCp composition is an optimum MMC for wider applications. Since it shows improved mechanical properties as expected by the aerospace industries [33,34].

The literature review reveals that most of the researchers concentrate on developing some 2D and 3D FE Models and simulating the milling process. From the earlier research, it is understood that 3D FE Models are comparatively more reliable and effective in predicting the cutting force data, chip formation process, chip characteristics, and machining-induced damages than 2D FE models. However, the 3D FEM developed so far is not so reliable and efficient in simulating the milling operation in MMCs. Since, it requires huge computation resources, more knowledge in Finite Element studies in developing 3D FEM, time, and complexity in the geometry of the modern tools. Moreover, there are no correlation studies on chip failure and chip characterization from an experiment Vs. FEM simulation particularly in 3D.

Therefore in this research work, slot milling experiments were done in aluminum nanocomposite, followed by the development of a 3D FEM in Abaqus/Explicit. The experimental and FEM simulation results were correlated for FEM validation. Moreover, this validated 3D FE Model is an effective and reliable virtual tool to assist in selecting the optimum machining parameter settings [35] to ease the slot milling process thereby ensuring the dimensional accuracy and quality of the components milled by minimizing the machining-induced damages such as crack formation and surface finish.

## METHODOLOGY

### Material Selection

In this research work, the aluminum nanocomposite (AA 7075 + 1.5% nSiCp) was fabricated by introducing the nano-sized SiC particles as reinforcement into the matrix of AA7075 aluminum alloy. The reinforced particles (nSiCp) used in this research work were in the 45-65 nm range. AA7075 is a matrix material that owns excellent mechanical properties such as less density, good thermal behavior, high tensile strength, and a better surface. The nano silicon carbide particles possess good mechanical behavior such as heat conductivity, good wear resistance, low thermal expansion coefficient, and good temperature resistance. Hence, SiC was used as the reinforcement material to enhance the mechanical properties of AA7075. The composition of the AA 7075 + 1.5% nSiCp can be referred from the articles of the co-author [31,32].

The aluminum nanocomposite is made up of a stir casting method (shown in Figure 1a) with five different AA7075 + nSiCp compositions and mechanical characterization studies were carried out by Prakash *et al.* [32]. The mechanical properties of the aluminum nanocomposite with the composition, of 985 grams of AA7075 + 15 grams of nSiCp (1.5% by weight) are comparatively outstanding. Therefore, based on the literature review [29,30] and the former research work carried out by the co-author, the suggested composition (AA 7075 + 1.5% nSiCp) was preferred for the current research work. The field emission scanning electron microscope (FESEM) image of the fabricated aluminum nanocomposite was taken using the CARL ZEISS (Model: Sigma with Gemini Column) FESEM equipment. This equipment with features such as a resolution of 1.5 nm, In lens Detector, SE2 detector, and BSD detectors is good enough to capture the surface topography of the fabricated MMC at the required resolution.

The captured FESEM image shown in Figure 1b reveals how SiC nanoparticles are distributed within AA7075 matrix material by Prakash *et al.* [32]. The fabricated aluminum nanocomposite is a very good alternative to steel. The former research carried out by the co-author reveals the enhancement in the mechanical properties, when AA7075 is reinforced with 1.5% nSiCp. The mechanical properties of AA7075 with 1.5% nSiCp are found to be excellent from the earlier studies [32].

## EXPERIMENTAL SETUP

The slot milling experiments were carried out in a BMV 51 TC24 vertical milling center with the machining parameters listed in Table 1. Figure 1c shows the experimental setup which comprises of milling center, tool, workpiece, and the mill tool dynamometer with a data-acquisition system. The TiAlN coated solid carbide end mill cutter is used for experiment studies which was supplied by Ultimate Machine Tools, Chennai, India. End Mill Tool – The CoroMill model, which was specially designed for milling composites, is used for this investigation [26]. Moreover, an

end mill cutter with a helix angle of $30^0$ and a point angle of $130^0$ to $140^0$ is selected for this experimental investigation as it is highly preferred by recent researchers and tool manufacturers [9,25,38]. The slot milling experiments were conducted with different cutting velocities and feed combinations presented in Table 1. However, the machining parameter values were selected based on the suggestions of the researchers and the information from the earlier investigations carried out by the authors. The key

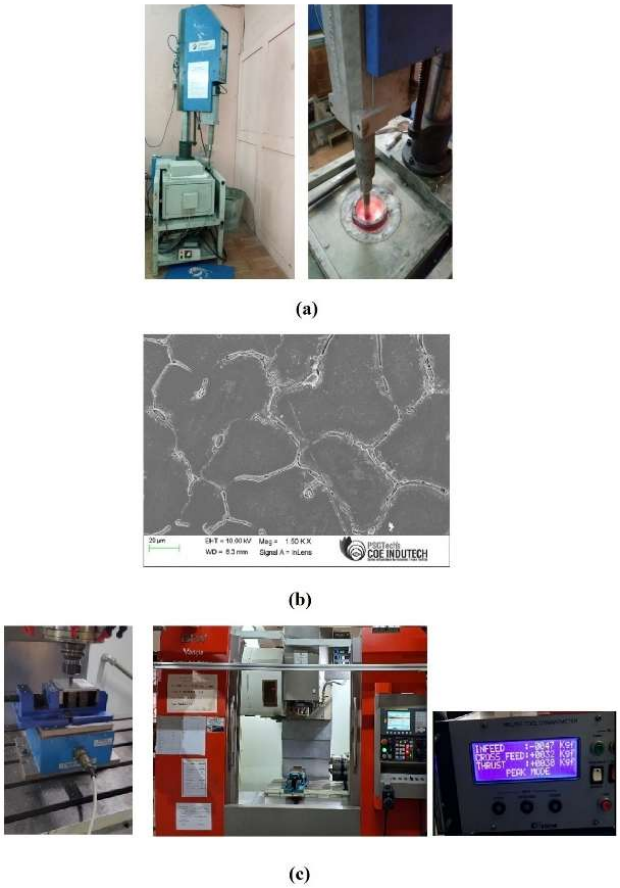


*Figure 1. a) Stir-casting with ultrasonic cavitation setup [25]; b) FESEM micrograph of the composite [25]; and c) milling experiment set up with Data - acquisition system.*

objective of this research was to perform chip morphological studies to evaluate, to report the chip formation and machinability of the aluminum nanocomposite, and to correlate with the 3D FEM simulation studies. This chip correlation study ensured the reliability of the developed 3D FEM. Hence, selecting the moderate and below moderate cutting velocity and feed rate combinations was mandatory for this current research work (given in Table 1). Since the chips obtained for these machining parameter combinations were good enough to visualize and categorize for correlating with FEM results [19,38]. However, the higher cutting velocity with a lower feed rate was preferred to minimize the cutting forces [9] whereas this cutting parameter combination produced very fragile and tiny chips that resembled dust particles. Moreover, these chips were found unsuitable for performing morphological studies. Cutting forces were recorded using a SYSCON mill tool dynamometer which was supplied by SYSCON Instruments Private Limited, Bangalore, India (shown in Figure 1c). The strain gauge-based milling dynamometer (Max Load capacity of 500 kgf, Model Name - SPL, Type - strain gauge) with full bridge component for each direction was utilized for this experimentation. The acquired analog signal was converted and communicated to the computer through an analog-digital converter, which was then displayed in the form of a graphical output to capture the cutting force data while performing experimental slot milling.

Table 1. Machining parameters settings for experimental slot milling of aluminum nanocomposite.

| Machining parameters | Values |
|---|---|
| Spindle speeds, N (rpm) | 250, 500, 1000, 1500 |
| Cutting Velocity, Vc (m/min) | 7.85, 15.7, 31.4, 47.1 |
| In feed rate, f (mm/min) | 50, 150, 250 |
| Slot depth (mm) | 1 |

### *Finite element analysis*

#### *FEA methodology*

In this research work, a Lagrangian 3D FEM was developed to simulate and visualize the slot milling operation in the aluminum nanocomposite using the ABAQUS FEA software [39]. 3D FE simulation trials were performed for different machining parameter combinations given in Table 2 and the critical cutting force, stress, and chip formation phenomenon were predicted (described in the results and discussion section). The milling simulation created by the 3D FEM technique helped in visualizing the interaction of the end mill and the MMC very effectively and provided insight into the machinability of the aluminum nanocomposite from a different perspective. Moreover, 3D FEM is the only effective technique to visualize the dynamic metal cutting process which involves the interaction of complex tool surfaces with workpieces [8].

#### *3D model of tool and aluminum nanocomposite.*

The three-dimensional model of the end mill tool with two flutes was modeled in CATIA V5 using the part module [40] (shown in Figure 2a) as per the tool nomenclature described elsewhere [26]. The 3D model of the four fluted end mill cutters was modeled in CATIA V5 and saved in the interactive graphics exchange system (IGES) format which was imported to ABAQUS to develop 3D FEM. The 3D equivalent homogeneous model ($25 \times 25 \times 10$) $mm^3$ of the aluminum nanocomposite was created as shown in Figure 2b using the part module in ABAQUS.

#### *3D finite element model*

The 3D FEM was developed by assembling and positioning the 3D model of the end mill cutter and the MMC. Furthermore, tool and MMC models were discretized with suitable element types and element numbers based on the requirement to simulate the machining process optimistically (the FE input details are given in Table. 2). Element mesh optimization (selection of suitable mesh

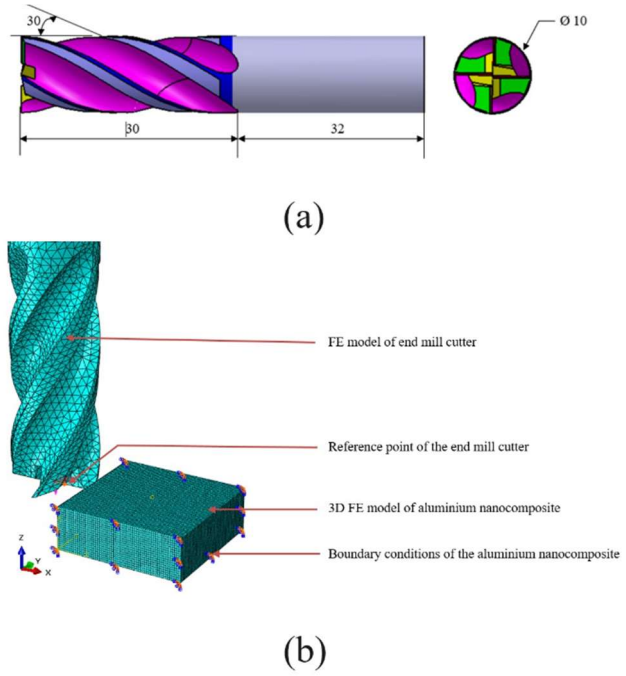


*Figure 2. a) Three-dimensional model of the solid carbide end mill cutter and b) three-dimensional finite element model of end milling aluminum nanocomposite.*

size) of the 3D FEM is mandatory to simulate the machining process effectively to compromise between the available computational resources, solving time and the efficiency & reliability of the FE results. The 3D model of the end mill tool was considered a rigid body [8,19,39] to reduce the computing efforts. Moreover, the mechanical properties of the mill tool were superior to the MMC, and in addition, tool wear studies were not in focus in the current research work which would be considered in our future investigations.

Table 2. 3D FEM-input data

| Workpiece | Aluminum nanocomposite |
|---|---|
| Tool | End Mill cutter - 10 mm diameter |
| Dimensions of workpiece (MMC) | 25 X 25 X10 mm |
| Element type for MMC | C3D8R |
| Number of elements in MMC | 50,000 |
| Number of nodes in MMC | 54,621 |
| Element size in MMC | 0.25 mm |
| Type of Element in end mill | C3D10M |
| Number of elements in end mill | 32,895 |
| Number of nodes in end mill | 49,665 |
| Element size in end mill | 1 mm |
| Total elements & nodes in 3D FEM | 82,895 & 1,04,286 |
| Friction factor | 0.6 & Coulomb friction [35] |
| Damage initiation | 1E-4 |
| Failure criteria | Johnson-Cook model |

The assumptions in developing the 3D FEM for performing slot milling simulation studies are as follows:

- The composite model developed for this current study is an equivalent homogeneous model (EHM).
- The 3D model of the twist drill is assumed to be a rigid body since tool wear is not considered in the current investigation to reduce computational efforts.
- Tool wear is not considered in this investigation, which is not the main focus of the study.
- In friction modeling the frictional stress developed in the tool-workpiece interaction zone during slot milling operation is proportional to the normal stress.
- Thermal issues are not considered as the temperature recorded during slot milling experimentation is less than 5 °C only, which is kept as our future scope of study.

### *Material modeling and failure criterion of AA 7075 + 1.5% SiC*

The fabricated MMC with the chemical composition listed in Table 3 shows excellent mechanical properties. Johnson's cook failure model available in the material model of the ABAQUS software was incorporated in the developed 3D FEM to simulate the plastic behavior of the aluminum nanocomposite. The Johnson-Cook (J-C) failure criterion (Eq. 1) was preferred for this investigation because it was good enough to predict the cutting forces, stress, chip morphology, flow stress, and plastic deformation for ductile materials and metals. It is widely used by researchers for machining simulation studies [26,41,42]. The features of the J-C parameters are as follows,

### *Advantages of the J-C failure model in the 3D FEM-based machining simulation [39]*

- The J-C failure model is best suited for materials that experience high strain rate, large strain, and larger deformation.
- It also considers plasticity, flow stress, work/strain hardening, and temperature softening of metallic materials.
- The J-C failure model is excellent for exhibiting the material behavior under dynamic (dynamic explicit) situations like machining simulation.
- Supports progressive degradation of material stiffness and removal of mesh elements by incorporating appropriate damage initiation and evolution factors. This assists in chip formation and separation in 3D FEM machining simulation.

### *Disadvantages and limitations of the J-C failure model in the 3D FEM-based machining simulation [39]*

- The seven parameters need to be determined for each structural material, which makes the investigation costlier and time-consuming.
- The solving time of the machining simulation using 3D FEM takes a long time.
- It is mandatory to correlate the simulation results with experimental results to be validated.

The J-C failure criterion is utilized to define the mechanical properties of the aluminum nanocomposite, J-C constitutive material parameters, and J-C damage parameters $d_1$ to $d_5$ (all given in Table 3) [42-44]. The damage evolution and element removal are initiated by the J-C damage initiation criterion. At the damage initiation parameter $d = 0.001$, it facilitates the FEM to activate chip

formation [35]. Enough preliminary trial simulation studies were carried out and appropriate damage initiation parameters were selected.

$$\sigma = (A + B\varepsilon^n)\left(1 + C\, ln\frac{\varepsilon_1}{\varepsilon_0}\right)\left[1 - \left(\frac{T-T_r}{T_m-T_r}\right)^m\right] \quad (1)$$

The constants *A*, *B*, *C*, *n*, *m*, and *T* are listed in Table 3.

### *Boundary conditions*

The loading conditions (cutting velocity and feed rate combination listed in Table 1) and the boundary conditions that prevailed in the real-time slot milling process were applied to the 3D FEM [24,25]. The aluminum nanocomposite-workpiece FE model was constrained for all degrees of freedom for the outer four sides and the bottom surface (as shown in Figure 2b). The tool was constrained for degrees of freedom except for feed direction (*X*-axis) and tool rotation axis (rotation along *Z*-axis). Furthermore, the feed rate and spindle speed values were given as input to the reference point which is created at the tip of the end mill cutter as shown in Figure 2b.

Table 3. Chemical composition, mechanical properties, J-C parameters, and damage criterion of aluminum nanocomposite [17,25].

| Composition of aluminum nanocomposite – AA7075 + 1.5% nSiCp (percentage by weight) [27,28] | | | | | | | | | |
|---|---|---|---|---|---|---|---|---|---|
| Cr | Mg | Zn | Cu | Si | Mn | Ti | Fe | SiC | Al |
| 0.2 | 2.4 | 5.7 | 2.0 | 0.3 | 0.1 | 0.1 | 0.22 | 1.5 | Bal |

| Mechanical properties of the composite [25] | | | |
|---|---|---|---|
| Specifications | Value(s) | Specifications | Value(s) |
| Modulus of elasticity, E (GPa) | 71 | Tensile strength (MPa) | 285.64 |
| Poisson's ratio | 0.27 | Yield strength (MPa) | 245.12 |
| Thermal expansion coefficient, (1/K) | 23.6 E-6 | Ultimate strength (MPa) | 260.56 |
| Thermal conductivity, k (W/mK) | 180 | Shear strength (MPa) | 150.53 |
| Specific heat (J/kg K) | 880 | Density of the composite (kg/m3) | 2790 |

| Johnson-Cook parameters [35] | | | | | | |
|---|---|---|---|---|---|---|
| *A* (MPa) | *B* (MPa) | *n* | *m* | *C* | Temperature (K) | Damage initiation |
| 251 | 1443 | 0.749 | 1.571 | 0.0166 | 305 | 0.001 |

| Damage parameters | | | | |
|---|---|---|---|---|
| $d_1$ | $d_2$ | $d_3$ | $d_4$ | $d_5$ |
| -0.77 | 1.45 | -0.47 | 0 | 1.60 |

The coulomb friction concept (sliding and sticking friction) was introduced in the developed 3D FEM which characterized the interaction between the tool and the aluminum nanocomposite (governed by Eq 2). This interaction behavior characterizes the frictional effect produced while performing slot milling operations in the MMCs [45]. The friction coefficient between the composite and end mill cutter was taken as 0.6 [8,42].

### *Interaction properties*

$$\tau_n = \mu\sigma_n \quad (2)$$

## RESULTS AND DISCUSSION

### *Cutting force*

The elevated cutting forces developed while machining the MMCs cause machining-induced damages such as surface roughness, dimensional inaccuracy, residual stress, internal cracks, etc. Moreover, the cutting force is the key parameter that influences more in chip formation, stress, chip morphology, and tool wear while performing slot milling operations in the aluminum nanocomposite. The machining accuracy, quality, and reliability of the machined components are to be ensured by minimizing the milling-induced damages by reducing these cutting forces. However, minimizing the cutting forces while milling is quite challenging, which creates interest for the researchers to investigate machinability studies of MMC. However, evaluating the exact magnitude of critical cutting forces is very difficult which depends on the experimental procedures and quality of the testing equipment utilized [8]. On the other hand 3D FEM technique is the only efficient method to predict these critical cutting forces by simulating the slot milling operation.

Figures 3a and 3b reveal a fluctuating pattern in the cutting force profile since the cutting edge angle varies with respect to the reinforced nano SiC particles while milling the aluminum nanocomposite. Whenever the cutting edge of the end mill interacts with reinforcement material (nano SiC particle) the magnitude of the cutting force increases since the nSiC particles are harder to break down while machining when compared to AA7075 [46]. Moreover, the AA7075 undergoes ductile failure whereas the SiC particle undergoes brittle failure [17]. The cutting force profile acquired from experimental and 3D FE simulations at *Vc* = 47.1 m/min and *f* = 150 mm/min is displayed in Figure 3b.

Figures 3c and 3d show the critical cutting forces generated for the corresponding cutting velocity and rate of feed (also listed in Table 4). Table 4 displays the cutting

feed (also listed in Table 4). Table 4 displays the cutting force components $F_x$, $F_y$, and $F_z$ for different cutting parameter combinations. It is also observed that the infeed force, $F_x$, and the cross-feed force, $F_y$ is comparatively

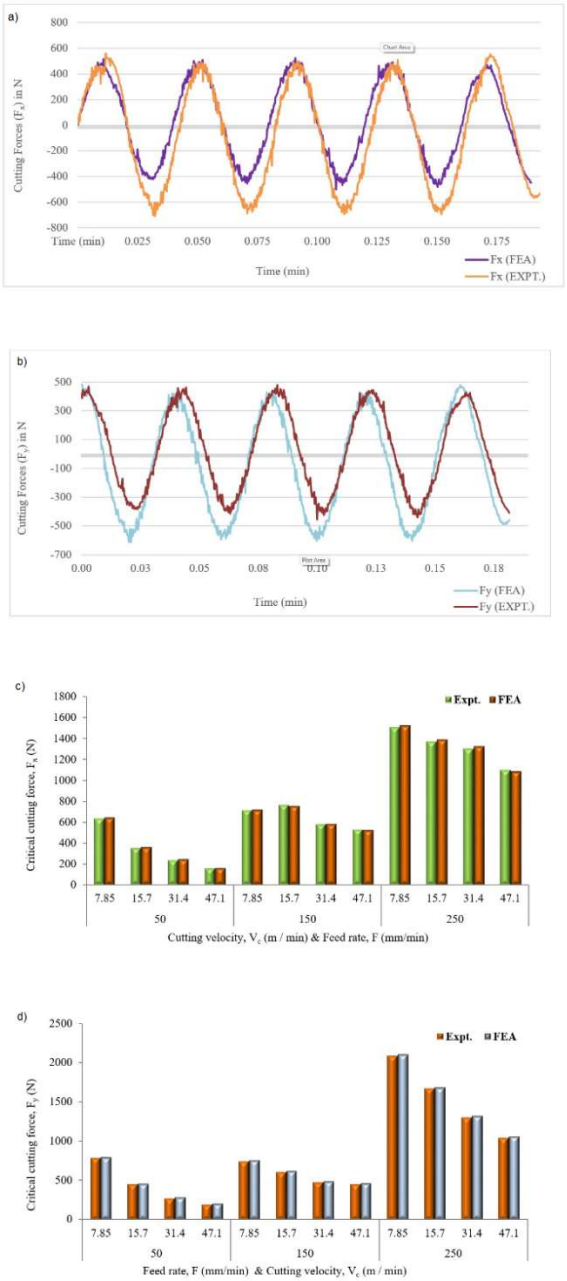


*Figure 3. a) Comparison of experimental and 3D FEM cutting force (Fx) during slot milling of aluminum nanocomposite when Vc = 47.1 m/min and f = 150 mm/min; b) comparison of experimental and 3D FEM cutting force (Fy) during slot milling of aluminum nanocomposite when Vc = 47.1 m/min and f = 150 mm/min; c) cutting velocity and feed rate vs. critical cutting force (Fx); and d) cutting velocity and feed rate vs. critical cutting force (Fy).*

higher than the thrust force, $F_z$. When the slot milling operation is carried out at a higher cutting velocity the cutting forces developed are minimal and vice-versa. Hence, it is highly recommended to perform the slot milling operation in aluminum nanocomposite at higher cutting velocity or lower feed/tooth to minimize the machining-induced damages caused due to critical cutting force [9]. The critical cutting force values captured from the experimental investigation and 3D FE simulation are correlated and the similarity error is found to be in the acceptable range [47]. Figure 3 shows the acceptable deviation of 10 to 15% in the correlation of 3D FE and experimental results which is mainly due to the tool run-out during cutting action [12].

### *Stress*

The shearing action of the end mill cutter when it interfaces with the MMC during the slot milling operation results in chip formation and material removal [25]. Hence, investigating the shear stress developed at the tool-workpiece interface region is vital, since it is the major influencer for chip formation, chip progression, and chip characteristics during the slot milling operation in the aluminum nanocomposite. The significance of the investigation on shear stress generation in the cutting zone is revealed in Figure 4a. The maximum shear stress ($S_{12}$) observed in the cutting zone is 175 MPa which effectively assists in the shearing of MMC.

3D FE simulation plots revealed that the von Mises stress obtained is 459 MPa (shown in Figure. 4 a) which is greater than the ultimate strength of the MMC listed in Table 3. The highest stress value of 459 MPa is observed in the cutting zone which is mainly due to the strength of the reinforcement material (nSiCp). Especially in the case of AA7075 reinforced with nanoparticles, more plastic deformation of the aluminum matrix is observed which is mainly due to the very high interaction frequency of the tool with the reinforcement particle. This phenomenon is lesser if the reinforcement particle size is larger comparatively by [15]. The highest stress value is observed at the root section of the milled chip (shown in Figure. 4a) which causes the chip to be in the yielding state for some time. This phenomenon results in the formation of curved-shaped chips, lamella structure, and twisted & rolled chip morphologies. Lamella structure in milled chips is observed for a few machining parameter combinations which is particularly due to the strained bands caused by the localized very high plastic von Mises stress during material removal.

### *Chip formation process in FEA*

The 3D FEM developed is utilized and the slot milling operation is simulated which is displayed in Figure 4b. The quality of the machined surface is a vital factor that influences the performance of the milled component from its application point of view. Achieving a good surface finish in the milling of nSiCp-reinforced MMCs very challenging since the formation of scratches and undercutting are quite common [46] which could be avoided only by paying special attention to the selection of suitable cutting velocity and feed. The 3D FEM is an excellent technique in revealing the metal cutting phenomenon to visualize if any machining-induced defect occurs.

Figure 4b reveals the ability of 3D FEM in simulating the chip formation phenomenon while performing slot milling in the aluminum nanocomposite. The effects of the selected cutting velocity and feed-on-chip morphology can

be visualized in 3D FE simulations. The chip morphology is mainly influenced by the shearing effect of the tool with the MMC, a variety of chips with different varieties [12] are obtained for respective cutting velocity and feed combinations which are visualized in Figure 5. The chip flows out of the workpiece through the flute region and it breaks into small curled chips. These small curled 'C' shaped chips are observed for most of the machining parameter combinations which is due to the effect of the interaction of the plastically deformed chip with the rake surface of the end mill cutter. However, the cutting velocity and feed highly influence the chip size, shape, and thickness. Moreover, nano-sized particle reinforcement enhances the yield property of the aluminum matrix [15,16] and thereby plastic deformation occurs easily resulting in the formation of 'C' and 'S' shaped curled chips which are witnessed in experimental as well as 3D FEM simulation (shown in Figures 4b).

### *Chip characteristics*

Chip morphology and chip formation pattern directly influence the dimensional accuracy, quality, and reliability of the milling operation. Therefore, the effects of cutting velocity and feed-on-chip generation are to be witnessed for a better understanding of chip formation and to facilitate the machining of defect-free components. Moreover, the tool geometry also significantly influences the chip characteristics. Figures 5 and 6 show samples of chips collected from experimental slot milling for various machining parameter combinations. It is witnessed that

Table 4. Critical cutting force data recorded for various cutting velocities and cutting feed combinations.

| Feed, $f$ (mm/min) | Cutting velocity, $V_c$ (m/min) | Critical cutting force (N) | | | | | |
|---|---|---|---|---|---|---|---|
| | | Infeed ($F_x$) | | Cross Feed ($F_y$) | | Thrust force ($F_z$) | |
| | | Expt. | FEA | Expt. | FEA | Expt. | FEA |
| 50 | 7.85 | 638 | 647 | 785 | 792 | 118 | 122 |
| | 15.7 | 353 | 361 | 451 | 462 | 69 | 73 |
| | 31.4 | 235 | 246 | 275 | 286 | 49 | 46 |
| | 47.1 | 157 | 162 | 196 | 206 | 39 | 34 |
| 150 | 7.85 | 716 | 719 | 746 | 759 | 167 | 156 |
| | 15.7 | 765 | 754 | 608 | 619 | 118 | 111 |
| | 31.4 | 579 | 586 | 481 | 493 | 59 | 57 |
| | 47.1 | 530 | 524 | 451 | 464 | 49 | 48 |
| 250 | 7.85 | 1511 | 1526 | 2080 | 2099 | 88 | 86 |
| | 15.7 | 1373 | 1392 | 1668 | 1679 | 59 | 55 |
| | 31.4 | 1305 | 1328 | 1305 | 1321 | 39 | 34 |
| | 47.1 | 1099 | 1086 | 1040 | 1062 | 29 | 27 |

collected are mostly 'C' shaped with a wider range of sizes, thickness, and length which is mainly influenced by the machining parameter combination selected for slot milling. The formation of a shorter 'C' shaped chip is predominant, which is mainly due to the reinforcement of nSiCp. The even distribution of nano SiC particles in the aluminum nanocomposite improves its ductile behavior, which causes plastic deformation during milling followed by the generation of curved and twisted chips. It is also observed that the chip thickness decreases while increasing the cutting velocity. However, chip thickness increases when the feed rate is increased. A chip with lamella structure is observed when $N$ = 250 rpm and $f$ = 250 mm/min since the thickness of the chip generated is comparatively higher. Moreover, the stress plots of the chips show highly strained bands across the chips which mainly contributes to the formation of lamellar structure in the milled chips. The localization of very high plastic Von Mises stress bands is the major contributor to these highly strained bands which results in lamella structure formation [15].

Figure 6a shows the magnified view (5X) of the milled chip at $f$ = 50 mm/min and $N$ = 250, 500, and 1000 rpm. The chips collected from the slot milling experiments for this particular feed rate mostly reveal very thin, curled, and 'C' shaped morphology. Cracks with saw tooth were observed in these "C' shaped chips which is because of the shearing action of the end mill cutter with the aluminum nanocomposite. Figure 6 (a) shows the magnified photographic images (5X) of the milled chip, $f$ = 150 mm/min and $N$ = 250, 500, 1000 rpm. In this case, the chip formation is short and thin shaped with lamella structure with cracks and saw tooth.

Mostly the milled chips possess 'C' or 'S' shaped morphology, which is due to the influence of the increased

feed rate when compared to the previous machining parameter conditions [12] for slot milling experimentation. Figure 6a displays the magnified image (5X) of the milled chip at $f$ = 250 mm/min. The milled chips show very good lamella structure at $N$ = 250 rpm which is due to the effect of higher chip thickness. At $N$ = 1000 and 1500 rpm, the chips show twisted and rolled-shaped morphologies.

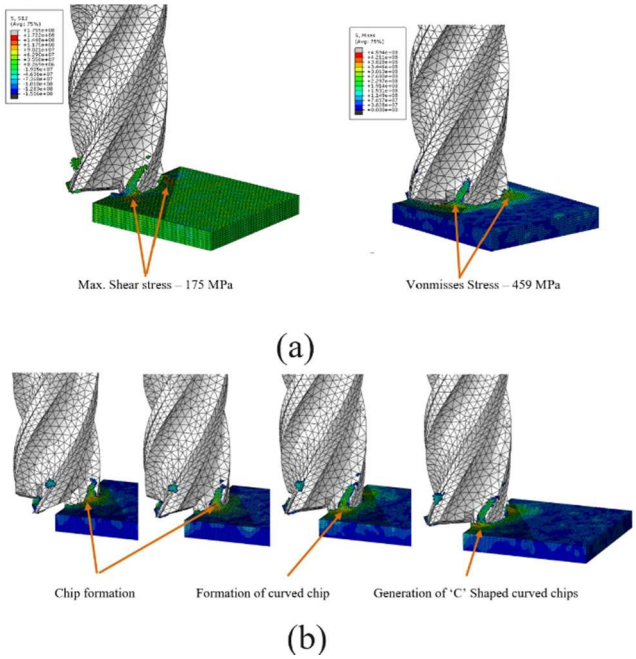


*Figure 4. a) Stress Plots from 3D FEA simulation when $V_c$ = 15.7 m/min and feed rate = 50 mm/min; b) 3D FEA slot milling simulation of chip formation at $V_c$ = 15.7 m/min, feed rate = 50 mm/min.*

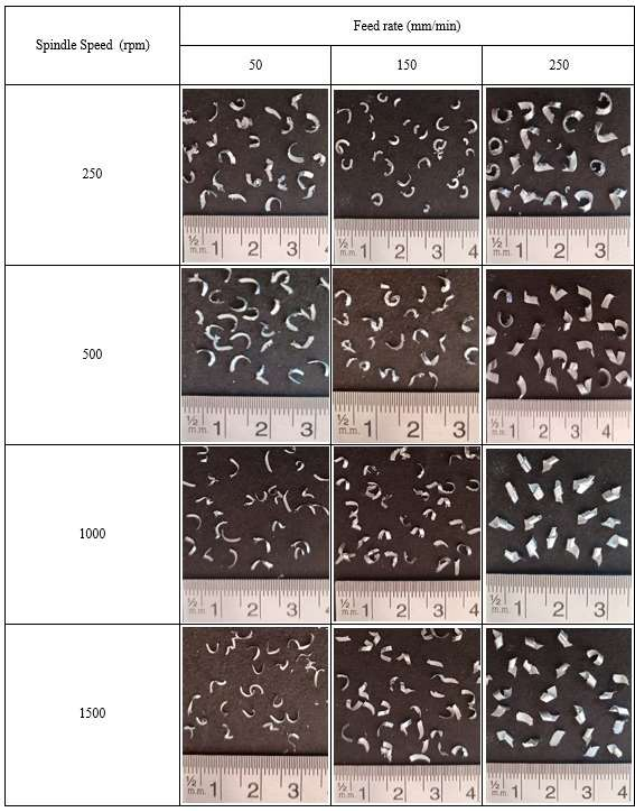


*Figure 5. Chip morphology of aluminum nanocomposite while slot milling with different cutting parameter combinations.*

The chips collected from experimental slot milling show good similarity when correlated with the chip plots captured from 3D FE simulation results as shown in the Figure 6b. The chip images obtained from experimental and 3D FE-based simulations show good similarity. The displayed

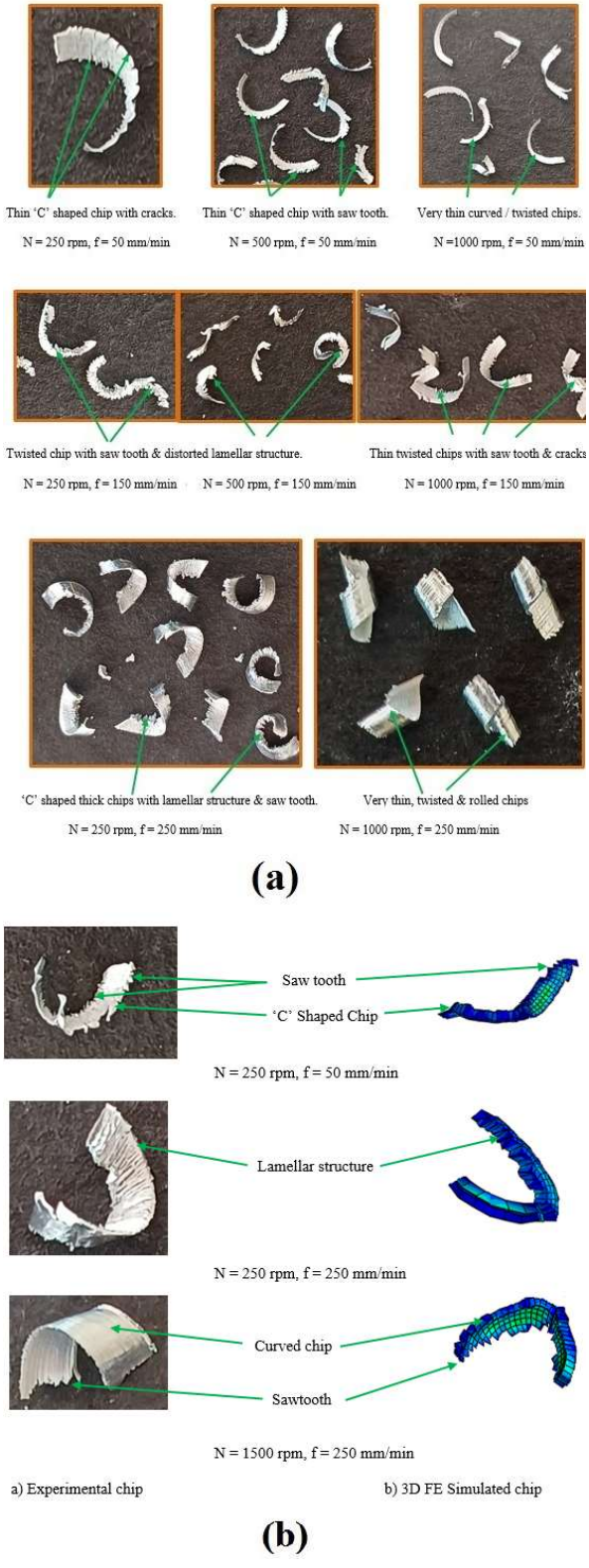


*Figure 6. a) Experimental chip characteristics at different spindle speeds and feed and b) comparison of chips morphology - experimental results vs. 3D FE simulation results*

images reveal the presence of cracks, lamella structure, and saw teeth. This ensures that 3D FEM-based simulations well exhibit the actual slot milling process and it is also significant in investigating the complex milling operation in a cost-effective and time-consuming way instead of arduous cutting experiments [11,48]. The chip images displayed below show the reliability and effectiveness of 3D FE simulation in predicting the chip morphology in slot milling of AA 7075 + 1.5% nSiCp nanocomposites.

The dimensions of the milled chip play a major role in enhancing the accuracy, surface finish, and quality of the machined component. The length of the milled chips for most of the cutting conditions is in the 5 to 8 mm range, which is observed from both experimental and 3D FEM simulation results. The cutting depth used in the current research is 1 mm and hence the width of the chips is uniform around 1 mm for all the machining conditions. The experimentation and 3D Fem results reveal that the cutting parameters such as spindle speed and feed rate do not influence on-chip dimensions much. However, the chip thickness varies with respect to cutting speed and feed rate. For higher cutting speeds the thickness of the chip reduces relatively and the chip is fragile.

### *Future Scope of Study*

This research work encourages the researchers and industry to focus more on developing optimistic and reliable 3D FE models to perform machining simulations, which could ease the machining process and make it cost-effective and time-saving. In addition, the 3D FEMs are also capable of estimating critical cutting force, chip characteristics, and cutting stress even for worn-out tools and complex tool geometries. Hence this research work can be extended in the future to investigate further with new tool geometries, MMCs, and other machining operations, which could provide an insight for the industries and researchers.

## CONCLUSIONS

The experimental and 3D FEM simulation studies of the slot milling operation were carried out and investigated in aluminum nanocomposite. The 3D FE simulation outcomes are compared with the experimental data for 3D FE model validation. The validated 3D FE model was utilized to perform simulation studies in slot milling of aluminum nanocomposites and it was found to be more reliable and accurate.

Experimental results show that critical cutting force (Fx and Fy ) rises when the cutting velocity is reduced. However, when cutting velocity is increased the reduction of critical cutting force is observed, critical cutting force recorded is Fy = 2080 N for Vc = 7.85 m/min and f = 250 mm/min. The low cutting feed and higher cutting velocity are suggested to minimize the milling-induced damages. The cutting force signals predicted by the 3D FEM correlates 85 to 90% with experimental data.

The maximum shear stress, S12 = 175 MPa, and von Mises stress, S = 459 Mpa, were observed at the tool-MMC interface region. The chip morphology studies disclose the mode of failure in the milled chips. The chip images captured from 3D FE simulations showed a good correlation with the milled chips. The correlation studies of experimental investigations and 3D FEM-based machining simulations prove the accuracy and reliability of the developed 3D FEM. This 3D FEM could assist researchers and industries in selecting appropriate machining parameter settings to achieve defect-free machining without any machining-induced damages. Moreover, it reduces the machining trials, time, and cost.

### *Acknowledgments*

The authors are extremely thankful to the Department of Production Engineering, Madras Institute of Technology, Chrompet for facilitating us with the required machinery and testing facility for this research work.

### *Nomenclature*

$A$ - yield strength of the material, (MPa)
$B$ - hardening modulus, (MPa)
C - strain rate sensitivity coefficient
D - material constant
f - feed rate, (mm/min)
$F_x$ - infeed force
$F_y$ - cross-feed force
$F_z$ - thrust force
$m$ - temperature sensitivity coefficient
N - spindle speed, (rpm)
$n$ - coefficients related to strain hardening, (MPa)
S - maximum Von Mises stress (MPa)
$T$ - temperature of the parts (◦C)
$T_r$ - ambient temperature (◦C)
$T_m$ - melting temperature (◦C)
$V_c$ - cutting velocity, (m/sec)

Greek symbols:

$\varepsilon$ - equivalent plastic strain
$\varepsilon_1$ - equivalent plastic strain rate, (S-1)
$\varepsilon_0$ - reference equivalent plastic strain rate, (S-1)
$\Sigma$ - flow stress, (MPa)
$\tau$ - shear stress, (MPa)
$\tau_n$ - frictional stresses, (MPa)
$\sigma_n$ - normal stresses, (MPa)
$\sigma$ - Johnson-Cook flow stress, (MPa)
$\sigma_1$ - maximum principal stress, (MPa)
$\mu$ - coefficient of friction

## REFERENCES

[1] Macke, B.F. Schultz, P. Rohatgi, Adv. Mater. Processes 170(3) (2012) 19-23. https://doi.org/10.31399/asm.amp.2012-03.p019.

[2] N. Shetty, S.M. Shahabaz, S.S. Sharma, S. Divakara, Shetty, Compos. Struct. 176 (2017) 790-802. https://doi.org/10.1016/j.compstruct.2017.06.012.
[3] D. Giugliano, N.K. Cho, H. Chen, L. Gentile, Compos. Struct. 218 (2019) 204-216. https://doi.org/10.1016/j.compstruct.2019.03.030.
[4] R. Bach, Aluminum in transport (2020). Available from: https://www.aluminumleader.com/application/transport/[accessed 16th August 2024]
[5] Y. Peng, H. Zhao, J. Ye, M. Yuan, L. Tian, Z. Li, Z. Wang, J. Chen, Compos. Struct. 288 (2022) 115425. https://doi.org/10.1016/j.compstruct.2022.115425.
[6] X.D. Nong, Y.L. Jiang, M. Fang, L. Yu, C.Y. Liu, Int. J. Heat Mass Transfer 108 (2017) 1374-1382. https://doi.org/10.1016/j.ijheatmasstransfer.2016.11.108.
[7] K. Palanikumar, N. Muthukrishnan, K.S. Hariprasad, Mach. Sci. Technol. 12(4) (2008) 529-545. https://doi.org/10.1080/10910340802518850.
[8] K. Giasin, A. Hodzic, V. Phadnis, S. Ayvar-Soberanis, Int. J. Adv. Manuf. Technol. 87(5) (2016) 2041-2061. https://doi.org/10.1007/s00170-016-8563-y.
[9] M. Aamir, K. Giasin, M. Tolouei-Rad, A. Vafadar, J. Mater. Res. Technol. 9(6) (2020) 12484-12500. https://doi.org/10.1016/j.jmrt.2020.09.003.
[10] M. Bhuvanesh Kumar, R. Parameshwaran, K. Deepandurai, S.M. Senthil, Trans. Indian Inst. Met. (2020). https://doi.org/10.1007/s12666-020-01960-6.
[11] W. Ma, R. Wang, X. Zhou, X. Xie, Proc. Inst. Mech. Eng., Part B 235(1-2) (2021) 265-277. https://doi.org/10.1177/0954405420932442.
[12] Davoudinejad, G. Tosello, P. Parenti, M. Annoni, Micromachines 8(6) (2017) 187. https://doi.org/10.3390/mi8060187.
[13] P. Raghuvaran, M. Suresh, S. Aakash, M. Balaji, K. Dinesh Kumar, S. H. Prasath, IOP Conf. Ser. Mater. Sci. Eng. 995 (2020). https://doi.org/10.1088/1757-899X/995/1/012040.
[14] K.H. Cui, C.Z. Ren, G. Chen, Key Eng. Mater. (589-590) (2013) 3-7. https://www.scientific.net/KEM.589-590.3.
[15] U. Usama, A. Hisham, H.A. Mustufa, M.M. Khan, H.A. Kishawy, Adv. Mech. Eng. 13 (2021). https://doi.org/10.1177/16878140211070446.
[16] U. Umer, M.H. Abidi, J.A. Qudeiri, H. Alkhalefah, Mater. Today: Proc. 44 (2021) 764-770. https://doi.org/10.1016/j.matpr.2020.10.679.
[17] L. Zhou, C. Cui, P. Zhang, Int. J. Adv. Manuf. Technol. 91 (2017) 1935-1944. https://doi.org/10.1007/s00170-016-9933-1.
[18] Prakash, K.S. Vijay Sekar, J. Balk. Tribol. Assoc. 23(3) (2017) 497-514.
[19] Prakash, A. Arockia Selvakumar, J. Prakash, AIP Conf. Proc. 3216(1) (2024) 040002. https://doi.org/10.1063/5.0226489
[20] A.F.V. Pedroso, N.P.V. Sebbe, R.D.F.S.Costa, M.L.S. Barbosa, R.C.M. Sales-Contini, F.J.G. Silva, R.D.S.G. Campilho, A.M.P. de Jesus, An Extended Review. J. Manuf. Mater. Process. 8(1) (2024) 37. https://doi.org/10.3390/jmmp8010037.
[21] S. Dodla, K.J. Kirpalani Idnani, A. Katyal, Mater. Today: Proc. (2021). https://doi.org/10.1016/j.matpr.2021.01.136.
[22] S. Deshmukh, G. Joshi, A. Ingle, D. Thakur, Mater. Today: Proc. 46 (2021) 8410-8416. https://doi.org/10.1016/j.matpr.2021.03.450.
[23] L. Zhang, Z. Wu, C. Wu, Q. Wu, Compos. B Eng. 241, (2022) 110023. https://doi.org/10.1016/j.compositesb.2022.110023.
[24] Prakash, K.S. Vijay Sekar, Adv. Sci., Eng. Med. 10(3) (2018) 308-312. https://doi.org/10.1166/asem.2018.2125.
[25] C. Prakash, K.S. Vijay Sekar, J. Braz. Soc. Mech. Sci. Eng. 40(6) (2018) 279. https://doi.org/10.1007/s40430-018-1195-4.
[26] C. Prakash, K.S. Vijay Sekar, IOSR J. Eng. (2018) 22-28. https://iosrjen.org/Papers/ICPRASET%202K18/surya/Volume%201/auto/5.%2022-28.pdf.
[27] C. Prakash, K.S. Vijay Sekar, Lect. Notes Mech. Eng. (2019) 81-89. https://doi.org/10.1007/978-981-13-1724-8_8.
[28] C. Prakash, K.S. Vijay Sekar, IOP Conf. Ser. Mater. Sci. Eng. (2021). https://doi.org/10.1088/1757-899X/1128/1/012050.
[29] C. Prakash, A. Arockia Selvakumar, K.S. Vijay Sekar, Mater. Today: Proc. (2023). https://doi.org/10.1016/j.matpr.2023.08.234.
[30] C. Prakash, Int. J. Interact. Des. Manuf. (2024). https://doi.org/10.1007/s12008-024-02089-2.
[31] J. Prakash, S. Gopalakannan, Silicon 13 (2021) 409-432. https://doi.org/10.1007/s12633-020-00434-0.
[32] J. Prakash, S. Gopalakannan, V.K. Chakravarthy, Silicon 14(4) (2022) 1683-1694. https://doi.org/10.1007/s12633-021-00979-8.
[33] H. Liu, W. Zhu, H. Dong, Ke. Yinglin, Mechatronics 46 (2017) 101-114. https://doi.org/10.1016/j.mechatronics.2017.07.004.
[34] R.K. Bhushan, Adv. Compos. Hybrid Mater. 4(1) (2021) 74-85. https://doi.org/10.1007/s42114-020-00175-z.
[35] Boughdiri, T. Mabrouki, R. Zitoune, K. Giasin, M.F. Ameur, Compos. Struct. 304 (2023) 116458. https://doi.org/10.1016/j.compstruct.2022.116458.
[36] T. Ozben, E. Kilickap, O. Çakır, J. Mater. Process. Technol. 198(1-3) (2008) 220-225. https://doi.org/10.1016/j.jmatprotec.2007.06.082.
[37] S. Deshmukh, G. Joshi, A. Ingle, D.S. Thakur, Mater. Today: Proc. 46(17) (2021) 8410-8416. https://doi.org/10.1016/j.matpr.2021.03.450.
[38] S.S. Babu, C. Dhanasekaran, G. Anbuchezhiyan, K. Palani, Eng. Res. Express. 4 (2022) 025036. https://doi.org/10.1088/2631-8695/ac7038.

[39] Simulia, Abaqus 6.14 User's Manual (2014) Dassault systems.
[40] CATIA V5R14, User Manual (2014) Dassault systems. https://www.maruf.ca/files/catiahelp/CATIA_P3_default.htm.
[41] T. Mabrouki, F. Girardin, M. Asad, J.F. Rigal, Int. J. Mach. Tools Manuf. 48 (2008) 1187-97. https://doi.org/10.1016/j.ijmachtools.2008.03.013.
[42] C. Prakash, J. Prakash, Proc. Inst. Mech. Eng., Part D (2024). https://doi.org/10.1177/09544070241254148.
[43] Johnson, W. Cook, Eng. Fract. Mech. 21(1) (1985) 31-48. https://doi.org/10.1016/00137944(85)90052-9.
[44] S. Rasaee, A.H. Mirzaei, D. Almasi, Bull. Mater. Sci. 43(1) (2020) 1-8. https://doi.org/10.1007/s12034-019-1987-x.
[45] J.Y. Sheikh-Ahmad, Textbook of Machining of Polymer Composites, Springer New York, NY (2009). https://doi.org/10.1007/978-0-387-68619-6.
[46] Yu, Z. He, J. Li, Int. J. Adv. Manuf. Technol. 124 (2023) 97-110. https://doi.org/10.1007/s00170-022-10476-w.
[47] Li, M. Liu, S. Zhao, Mach. Sci. Technol. 25(4) (2021) 558-584. https://doi.org/10.1080/10910344.2020.1855651.
[48] C. Prakash, J. Prakash, Arch. Metall. Mater. 70(2) (2025) 583-600. https://doi.org/10.24425/amm.2025.153459.

PRAKASH CHAKRAPANI[1]

PRAKASH JAYARAMAN[2]

[1]Department of Automobile Engineering, School of Engineering and Technology, Surya Group of Institutions, Anna University, Tamilnadu, India.

[2]Department of Mechanical Engineering, School of Engineering and Technology, Surya Group of Institutions, Anna University, Tamilnadu, India.

NAUČNI RAD

# GLODANJE OTVORA NA PLOČAMA OD LEGURE AA7075 POJAČANE NANOČESTICIMA SILICIJUM-KARBIDA – EKSPERIMENTALNI PRISTUP I MODELOVANJE KONAČNIM ELEMENTIMA

*U trenutnom trendu, industrije radije optimizuju procese obrade koristeći tehnike simulacije obrade zasnovane na konačnim elementima. Legura aluminijuma 7075 (AA7075) ojačana nanočesticama silicijum-karbida se koristi u industriji jer pokazuju dobra fizička i mehanička svojstva. Glodanje otvora je suštinska operacija mašinske obrade za pretvaranje komponente u projektovani oblik i veličinu. Međutim, potrebno je odlično znanje u odabiru odgovarajućih parametara obrade, kao što su brzina rezanja, pomak i materijal reznog alata, kako bi se osigurao kvalitet glodanih komponenti. U ovom istraživačkom radu, operacija glodanja otvora je izvedena na pločama uzorka od AA7075 obogaćenom nanočesticama silicijum-karbida do 1,5% težine. 3D model konačnih elemenata (3D FEM) je razvijen korišćenjem softvera ABAQUS za simulaciju operacija glodanja otvora da bi se razumeo uticaj parametara obrade na sile rezanja, formiranje strugotine i morfologiju strugotine. Sile rezanja predviđene 3D FEM modelom koreliraju 85% do 90% sa eksperimentalnim podacima. Maksimalni napon smicanja od 175 MPa i Fon Mizesov napon od 459 MPa primećeni su na interfejsu alat-obradak. Ovaj validirani 3D FEM olakšava vizualizaciju i istraživanje procesa glodanja i pomaže u odabiru odgovarajućih postavki parametara obrade. Prikazani su efekti brzine rezanja na sile rezanja, karakteristike strugotine, naprezanje i formiranje strugotine.*

*Ključne reči: Aluminijumski nanokompozit, glodanje otvora, 3D FEM, sile rezanja, morfologija strugotina.*